Research Article

Lei Zheng#, Qianfan Zhang#, Hongguang Lian#, Wenli Wang, Liangsheng Li, Zekun Zhen, Ziyan Li, Lingdan Zhao, Tingting Zhang, Bin Zheng, Chao Wang, Wei Zhang, Jinkun Wen*, and Xinhua Zhang*

The LyP-1 cyclic peptide modified mesoporous polydopamine nanospheres for targeted delivery of triptolide regulate the macrophage repolarization in atherosclerosis

https://doi.org/10.1515/ntrev-2024-0022
received December 15, 2023; accepted April 3, 2024

Abstract: Atherosclerosis (AS) is a chronic inflammatory disease that leads to the formation of atherosclerotic plaques in arterial walls, which can eventually result in cardiovascular diseases. It has been confirmed that the imbalance in the polarization of M1-type pro-inflammatory and M2-type anti-inflammatory macrophages in AS plaques is closely related to plaque instability and the development of cardiovascular diseases like AS-related heart and cerebrovascular diseases. Triptolide (TP) is a promising drug for the treatment of AS due to its anti-inflammatory and anti-proliferative effects. However, its poor solubility and lack of specificity limit its clinical application. We developed a targeted delivery system for TP to M1-type macrophages using mesoporous polydopamine (MPDA) nanospheres modified with the LyP-1 peptide. We then observed the performance of this targeted delivery system and explored its regulatory effects on macrophage polarization in AS. The results showed that the LYP-1-modified MPDA-TP delivery system had an average encapsulation rate of 66.5%, a drug loading capacity of 4.5%, and an average diameter of 250 nm. It exhibited excellent targeting ability and drug release rate towards target cells. LYP-MPDA-TP was capable of inhibiting the proportion of M1 macrophages induced by oxidized low-density lipoprotein stimulation in mouse macrophages, promoting apoptosis in M1-type macrophages significantly, and demonstrating a significant inhibitory effect on AS in experimental animals. The LYP-1 peptide-modified MPDA delivery system provides a new approach for TP treatment of AS and an important theoretical basis and methodological reference for the design of targeted delivery systems for anti-AS nanoparticles.

Keywords: LYP-1 cyclic peptide, mesoporous polydopamine nanospheres, targeted delivery of triptolide, atherosclerosis

# These authors contributed equally to this work and should be considered first co-authors.

*** Corresponding author: Jinkun Wen,** Department of Biochemistry and Molecular Biology, Key Laboratory of Neural and Vascular Biology, Ministry of Education, Hebei Medical University, 361 Zhongshan East Road, Shijiazhuang 050017, China, e-mail: wjk@hebmu.edu.cn
*** Corresponding author: Xinhua Zhang,** Department of Biochemistry and Molecular Biology, Key Laboratory of Neural and Vascular Biology, Ministry of Education, Hebei Medical University, 361 Zhongshan East Road, Shijiazhuang 050017, China; Institution of Chinese Integrative Medicine, Hebei Medical University, 361 Zhongshan East Road, Shijiazhuang 050017, China, e-mail: 18200814@hebmu.edu.cn, tel: +86-139-3387-0526
Lei Zheng: Department of Biochemistry and Molecular Biology, Key Laboratory of Neural and Vascular Biology, Ministry of Education, Hebei Medical University, 361 Zhongshan East Road, Shijiazhuang 050017, China; Institution of Chinese Integrative Medicine, Hebei Medical University, 361 Zhongshan East Road, Shijiazhuang 050017, China; Central Laboratory, Harrison International Peace Hospital, 180 Ren Min East Road, Hengshui 053000, China
Qianfan Zhang: Chongqing Institute of Green and Intelligent Technology, Chinese Academy of Sciences, Chongqing, 400714, China; School of Pharmacy and Bioengneering, Chongqing University of Technology, Chongqing, 400054, China
Hongguang Lian, **Zekun Zhen**, **Ziyan Li**, **Lingdan Zhao**, **Tingting Zhang**, **Bin Zheng:** Department of Biochemistry and Molecular Biology, Key Laboratory of Neural and Vascular Biology, Ministry of Education, Hebei Medical University, 361 Zhongshan East Road, Shijiazhuang 050017, China
Wenli Wang: Department of Biochemistry and Molecular Biology, Key Laboratory of Neural and Vascular Biology, Ministry of Education, Hebei Medical University, 361 Zhongshan East Road, Shijiazhuang 050017, China; Institution of Chinese Integrative Medicine, Hebei Medical University, 361 Zhongshan East Road, Shijiazhuang 050017, China
Liangsheng Li: Chongqing Institute of Green and Intelligent Technology, Chinese Academy of Sciences, Chongqing, 400714, China
Chao Wang: Geriatric Key Laboratory, Hebei General Hospital, 348 Heping West Road, Shijiazhuang 050057, China
Wei Zhang: Institution of Chinese Integrative Medicine, Hebei Medical University, 361 Zhongshan East Road, Shijiazhuang 050017, China

1 Introduction

Atherosclerosis (AS) is a progressive inflammatory disease and a leading cause of coronary heart disease, stroke, and peripheral vascular disease [1–3]. Studies have revealed that during the early stages of AS development, monocytes within the arterial intima differentiate into pro-inflammatory M1 macrophages, which locally amplify the inflammatory response and engulf lipoproteins in the intima, resulting in the formation of foam cells and the initiation of early atherosclerotic lesions [4]. Macrophages, including foam cells, have been found to play significant roles in all stages of AS by releasing pro-inflammatory mediators and inducing endothelial injury, particularly in the early stages of AS formation [5]. It has been established that an imbalance between pro-inflammatory M1 macrophages and anti-inflammatory M2 macrophages in AS plaques is closely associated with plaque instability and the development of AS-related cardiovascular and cerebrovascular diseases [6–8]. Studies have demonstrated that pro-inflammatory M1 macrophages can release various pro-inflammatory factors, such as TNFα, IL-1β, IL-6, and recruit monocytes and macrophages to the enriched plaque area, further exacerbating the inflammatory progression of vascular plaques [9]. Therefore, effective early interventions targeting the inhibition of pro-inflammatory M1 macrophages and the reduction of the amplification effect of pro-inflammatory factors within the inflammatory region may contribute to the concept of "preventing and controlling AS in its early stages" [5,10].

Currently, traditional lipid-lowering therapies and immunotherapies have limitations in suppressing the abnormal aggregation of AS macrophage cells [11–13]. In recent years, extensive research on traditional Chinese medicine in the fields of medical biology and clinical studies has demonstrated the potential clinical applications of various active monomers derived from Chinese herbal medicine for the treatment of AS [14,15]. *Tripterygium wilfordii*, for instance, has been found to exert anti-atherosclerotic effects by inhibiting the expression of inflammatory factors [16]. This is attributed to the ability of its active components to suppress the production of inflammatory transmitters, cytokines, and chemokines during the early stages of chronic inflammation in AS, thereby highlighting its promising prospects for application in AS treatment [16]. However, limitations such as poor solubility, short half-life in the body, and potential hepatotoxicity and nephrotoxicity have been observed in the application of *Tripterygium wilfordii lactone*, restricting its clinical utilization [16].

To address the limitations associated with the delivery of active monomers from traditional Chinese medicine, various carriers have been developed in recent years for *in vivo* drug delivery. Among these carriers, nanoparticles, exemplified by mesoporous polydopamine (MPDA) nanospheres, possess unique advantages in drug delivery due to their capacity for modification with different peptides tailored to the characteristics of distinct diseases [10,17]. This allows for targeted delivery and efficient drug enrichment, consequently enhancing efficacy while minimizing toxicity. Particularly crucial is the identification of appropriate antigens specifically expressed in early AS plaques, along with the corresponding targeted binding peptides, which can be employed to construct lipid nanoparticles for targeted drug delivery. Previous studies have shown that under physiological conditions, P32 (also known as the binding protein of LYP-1 peptide) is highly conserved in all tissues, while its expression is specifically increased in tumor tissues, as well as in macrophages and foam cells associated with AS [18]. It has been utilized as a targeted peptide for AS imaging diagnosis [19,20]; however, limited research has explored its combination with MPDA for AS-targeted drug delivery.

Therefore, the objective of this study is to modify the LyP-1 cyclic peptide onto MPDA and employ it as a delivery system to encapsulate triptolide (LYP-MPDA-TP) for targeted delivery. The aim is to achieve precise treatment of AS by regulating macrophages and foam cells in a targeted manner.

2 Methods

2.1 Cell lines

The murine RAW 264.7 cell line was obtained from Zhong Qiao Xin Zhou Biotechnology (ZQXZ Biotechnology, Shanghai, China). Female ApoE$^{-/-}$ mice (6 weeks old) were acquired from the Experimental Animal Center of Chinese Academy of Medical Sciences (Beijing, China). These mice were housed in a dedicated pathogen-free animal facility at the Institute of Department of Biochemistry and Molecular Biology, Key Laboratory of Neural and Vascular Biology, Ministry of Education, Hebei Medical University, with unrestricted access to food and water. All animal procedures were conducted in compliance with institutional ethics regulations and guidelines on animal welfare and received approval from the Animal Ethics Committee at the Hebei Medical University.

2.2 Synthesis of MPDA nanoparticles

The MPDA nanoparticles were synthesized by one-pot method as the previous reference. Briefly, 60 mL H_2O and

60 mL ethanol were mixed, and then 0.3 g Pluronic ® F127 (F127) and 0.3 g 1,3,5-trimethylbenzene were added. 85 mL tris(hydroxymethyl) aminomethane solution was dissolved to the mixture after stirring and dissolving. Then, 55 mg dopamine hydrochloride was added for 24 h at room temperature. The synthesized MPDA nanoparticles was obtained by high-speed centrifugation. The collected MPDA nanoparticles were then characterized by transmission electron microscope (TEM) and scanning electron microscopy (SEM).

2.3 Preparation of LYP-MPDA-TP nanoparticles

10 mg MPDA nanoparticles were resuspended in 20 mL H_2O followed by ultrasonic treatment. For the synthesis of MPDA-PEG nanoparticles, 20 mg 4 branched-PEG-NH_2 were added to the above solution and stirred overnight. The targeted LyP-1 Cyclic Peptide (CGNKRTRGC) were purchased from the Shanghai Topscience Co., Ltd. Then, 5 mg MPDA-PEG nanoparticles, 1 mg LyP-1 Cyclic Peptide, 4 mg EDC·HCl, and 4 mg Sulfo-NHS were resuspended in 2 mL H_2O and stirred for 24 h to obtain the LYP-MPDA-TP nanoparticles.

Three milligrams of different nanoparticles were suspended in 1 mL of DI water with 0.5 mg TP overnight. Then, the products were ultrafiltration centrifuged (MWCO 10kD) and the MPDA-TP and LYP-MPDA-TP were obtained.

2.4 *In vitro* safety evaluation

Cytotoxicity evaluations of PBS, free MPDA nanoparticles, and LYP-MPDA nanoparticles were performed using RAW264.7 cells and 3-[4,5-dimethylthiazol-2-yl]-2,5 diphenyl tetrazolium bromide (MTT) assays. Cells were seeded in 96-well plates at a density of 10^5 cells/mL. After 24 h of incubation, the media were replaced with fresh media containing different concentrations (0.5, 2.5, and 12.5 mM) of MPDA nanoparticles or LYP-MPDA nanoparticles. Following an additional 24 h of incubation, the media were substituted with DMEM containing MTT. The survival rate of the cells was determined using an MTT enzyme-linked immunometric meter, and data were analyzed using SoftMax Pro 5.4.1. Statistical analysis was performed using GraphPad Prism 6.

2.5 Cellular uptake and intracellular drug release

Cellular uptake and intracellular drug release experiments were conducted using macrophages, oxidized low-density lipoprotein (oxLDL)-treated macrophages. Cells were seeded and incubated at 37°C for 24 h. Subsequently, the media were replaced with fresh media containing Cy5 nanoparticles and LYP-Cy5 nanoparticles, respectively. After an additional 1, 2, 4, 6, and 12 h of incubation, the cells were washed three times with PBS buffer and fixed with paraformaldehyde for 15 min. After an additional three PBS washes, the cells were observed using BD FACSCanto II Flow Cytometer. The amount of loaded TP onto the NPs is calculated according to the standard UV−Vis curve of TP. The prepared LYP-MPDA-TP were suspended at 37°C in 5 mL PBS solution with pH 7.4 and pH 5.5, respectively. At determined time points (0, 0.5, 1, 2, 4, 8, 16, 24, 36, and 48 h), 1 mL of suspension was collected for UV−Vis analysis.

2.6 Cell apoptosis assay *in vitro*

To assess cell viability and apoptosis, RAW264.7 cells were exposed to a culture medium containing 20 μg/mL of oxLDL in the presence of different treatments: saline, MPDA, LYP-MPDA, TP, MPDA-TP, and LYP-MPDA-TP. These treatments were administered at varying concentrations of TP (1.25, 5, and 20 μM) for a duration of 24 h.

Apoptosis rates were measured after a co-treatment period of 6 h. The cells were processed according to the instructions provided by the manufacturers of the fluorescein isothiocyanate (FITC) Annexin V Apoptosis Detection Kit I. Briefly, the cells were suspended in 100 μL of binding buffer and mixed with 10 μL of annexin V-FITC and 10 μL of propidium iodide. After a 15-min incubation, an additional 400 μL of binding buffer was added, and the cells were analyzed using a flow cytometer to determine the apoptosis rates. FlowJo software (version 7.6.1) was used for data analysis.

2.7 Western blot

RAW264.7 cells were exposed to the culture medium containing 50 μg/mL of oxLDL and various treatments: saline, MPDA, LYP-MPDA, TP, MPDA-TP, and LYP-MPDA-TP. The treatments were applied at different concentrations of TP (1.25, 5, and 20 μM) for 24 h. After the incubation period, the cells were homogenized in RIPA buffer supplemented with protease inhibitors. The protein content was normalized using a bicinchoninic acid assay. Protein lysates (50–100 μg) from the cell samples were separated on a 10% sodium dodecyl sulfate polyacrylamide gel electrophoresis gel under reducing conditions and transferred to polyvinylidene fluoride (PVDF) membranes. The PVDF membranes were

then incubated overnight at 4°C with primary antibodies specific to the target proteins, including Caspase 8, Bcl-2, Cyto-C, Caspase 9, Caspase 3, and GAPDH. Subsequently, the membranes were incubated with a secondary antibody (goat anti-rabbit) for 1 h. The expression levels of the proteins were analyzed using an Alphalmag system.

2.8 Construction of AS in ApoE$^{-/-}$ mice

Female ApoE$^{-/-}$ mice, aged 6 weeks, were fed a high-fat diet comprising 21.2% lard, 49.1% carbohydrate, 19.8% protein, and 0.2% cholesterol for a duration of three months to induce AS. At the end of the treatment period, six mice were euthanized, and the extent of pathological changes was evaluated by measuring the lesion area of the aorta from the heart to the iliac bifurcation. Confirmation of atherosclerotic plaque formation was achieved through hematoxylin–eosin (H&E) staining performed on the aortic root.

2.9 *In vivo* therapeutic efficacy study

Female ApoE$^{-/-}$ mice at 6 weeks of age were randomly and blindly divided into four groups (n = 7): a control group (saline) and three treatment groups (TP, MPDA-TP, and LYP-MPDA-TP). These mice were subjected to a high-fat diet, identical in composition to the aforementioned diet, for a continuous period of three months. After the first month of high-fat diet treatment, the mice in each group received intravenous administrations of saline, TP, MPDA-TP, and LYP-MPDA-TP once a week at a dosage of 2 mg/kg TP (except for the saline-treated group) for an additional two months. Following the 2-month administration period, all mice were euthanized, and atherosclerotic plaques from ten mice in each group were collected for H&E staining. Imaging techniques were employed to evaluate the therapeutic efficacy of the different formulations. Furthermore, quantitative analysis of the atherosclerotic plaque was performed using Image-Pro Plus 6.0 software.

2.10 Histological study on aorta tissues

For histological analysis, the aortic root from mice in the various treatment groups were collected and subjected to H&E staining.

2.11 Statistical analysis

Statistical analysis was conducted using one-way analysis of variance (ANOVA) and two-way ANOVA. Statistical significance was denoted by $^{*}P \le 0.05$, $^{**}P \le 0.01$, and $^{***}P \le 0.001$. All data were presented as the mean value ± standard deviation of independent experiments.

3 Results

3.1 Synthesis and characterization of different nanoparticles

Different nanoparticles were synthesized by using a one-pot method, and the hollow mesoporous nanoparticles were collected and detected by using the TEM and SEM. As shown in Figure 1a–c, the particle size of LYP-MPDA-TP was approximately 250 nm. This indicated that the particle is suitable for delivering the TP to the cells. The zeta potential measurement results demonstrated that MPDA and LYP-MPDA carries more negative charges (Figure 1d), revealing the negatively charged TP filling the hollow mesoporous nanoparticles.

3.2 Selective uptake of LYP-MPDA-TP *in vitro*

The cell targeting efficacy of the LYP-MPDA-TP is crucial for delivering the TP to the macrophage. The tumor-homing peptide LyP-1 can bind to the protein P32, which is highly expressed in tumor tissues. It has been utilized as a targeted peptide LyP-1 for AS in many studies. Therefore, we modified the LYP-1 cyclic peptide onto the MPDA as a delivery system of TP for treating AS. We first examined the RAW264.7 cells targeting efficiency of the MPDA with the targeting peptide. Compared with the control group, the MPDA coupled with LYP-1 cyclic peptide showed a considerably higher density of internalized nanocomplexes in the Flow cytometry after 1–12 h of incubation (Figure 2a). Significantly, the free MPDA nanoparticles and LYP-MPDA nanoparticles showed no cell cytotoxicity (Figure 2b). In addition, the cumulative release of TP from LYP-MPDA-TP substrate was investigated. The release amount of TP from under pH 7.4 was less than that under acidic pH environment (pH = 5.5). The TP release basically arrived at the peak after 16 h (Figure 2c).

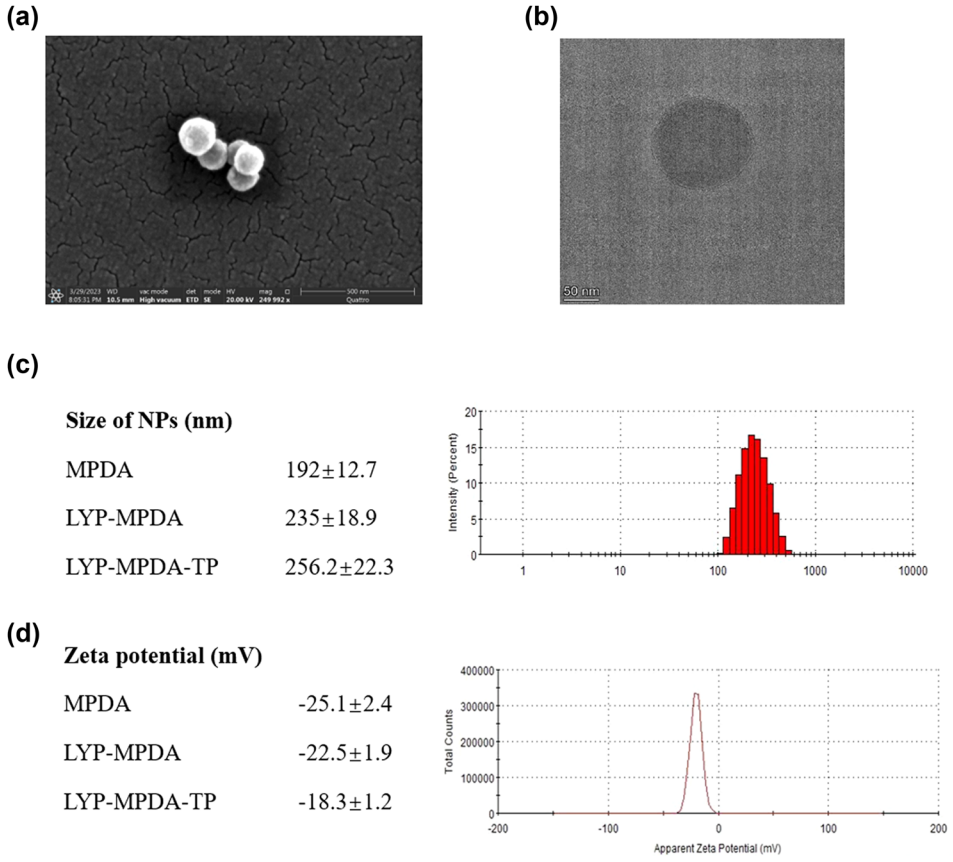

Figure 1: Characterization of the nanoparticles. (a) SEM image of LYP-MPDA-TP. (b) TEM image of LYP-MPDA-TP. (c) Average diameter of the MPDA, LYP-MPDA, and LYP-MPDA. (d) Zeta potential of MPDA, LYP-MPDA, and LYP-MPDA in H_2O.

3.3 The impact of LYP-MPDA-TP on oxLDL-induced macrophage polarization

To examine the influence of different TP formulations on macrophage polarization, mouse RAW264.7 macrophages were co-cultured with oxLDL (50 μg/mL) and various formulations (saline, TP, MPDA-TP, and LYP-MPDA-TP) for 24 h. Subsequently, the expression levels of phenotypic markers iNOS for M1 macrophages and Arg1 for M2 macrophages were assessed. Following oxLDL treatment, both mRNA and protein levels of the M1 marker iNOS in macrophages were significantly elevated compared to the control group (Figure 3a and c), and inflammatory cytokines which were associated with M1 polarization, including TNF-α, IL-1β, and MCP1, also exhibited substantial increases compared to the control group (Figure 3g–i). Conversely, the protein expression of the M2 marker Arg1 was significantly reduced after 24 h of oxLDL treatment (Figure 3b, c and e), while alterations in M2-related cytokines IL-10 and TGF-β were insignificant (results not shown). Remarkably, treatment with different TP formulations led to a significant reduction in the expression levels of the M1 marker iNOS in mouse macrophages at both the mRNA and protein levels, with LYP-MPDA-TP demonstrating the most pronounced inhibition (Figure 3a, c and d). Further experiments showed that the level of inflammatory cytokine TNF-α and IL-1β which were associated with macrophage M1 were inhibited after the treatment of all different TP formulations, with LYP-MPDA-TP exerting the strongest inhibition on these factors (Figure 3g–i). Moreover, TP formulations induced substantial changes in the expression of M2 anti-inflammatory marker proteins and their secreted cytokines (Figure 3b, c, e and i). Collectively, these findings suggest that LYP-MPDA-TP effectively suppresses oxLDL-induced polarization of mouse macrophages toward the pro-inflammatory M1 phenotype. Consequently, it reduces the release of pro-inflammatory factors by oxLDL-stimulated macrophages, thereby displaying potential for early intervention in AS lesions.

3.4 The influence of LYP-MPDA-TP on oxLDL-induced apoptosis in mouse macrophages

Subsequently, we investigated the impact of different TP formulations on oxLDL-induced apoptosis in mouse macrophages.

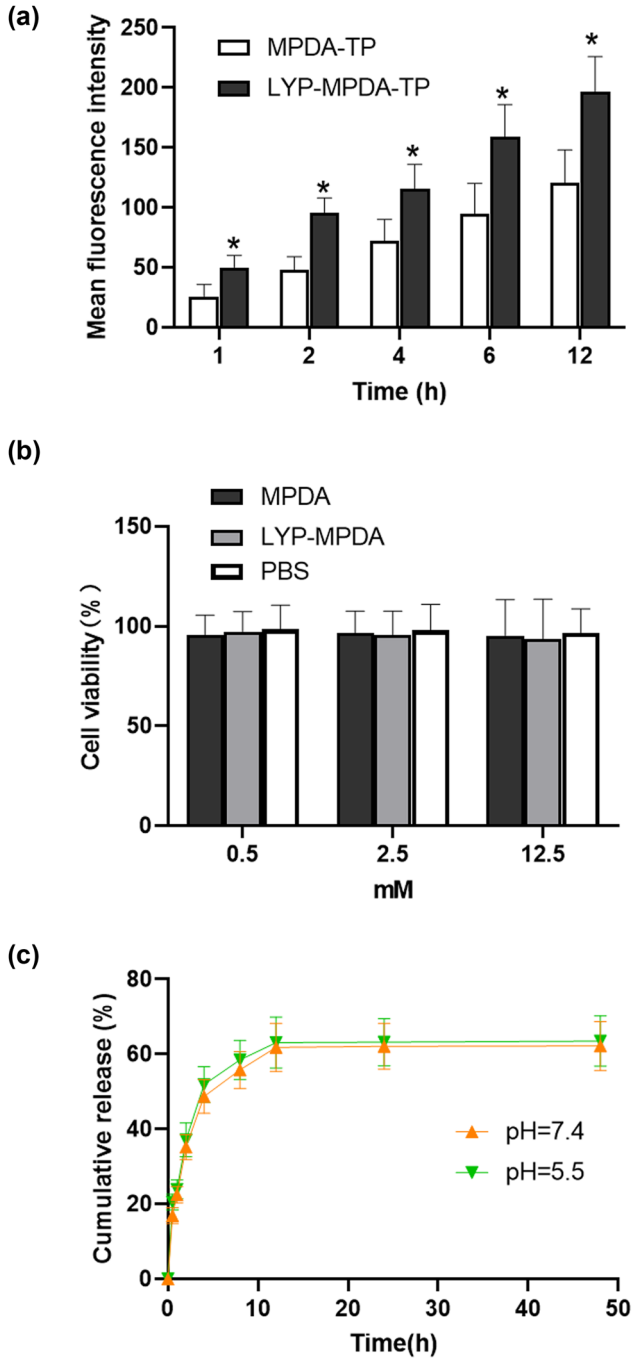

Figure 2: Analysis of cellular uptake, cell cytotoxicity, and drug release of the different nanoparticles. (a) *In vitro* cellular uptake analysis in RAW264.7 cell line at different time points. (b) Viability of RAW264.7 cells in response to the nanoparticles treatment. (c) The cumulative drug release of TP under pH 7.4 and 5.5 at different time points. *$P < 0.05$.

Mouse RAW264.7 macrophages were co-cultured with oxLDL (50 μg/mL) and diverse formulations (saline, MPDA, LYP-MPDA, TP, MPDA-TP, LYP-MPDA-TP) for 24 h. Flow cytometry was used to assess macrophage apoptosis, while western blot analysis was performed to detect apoptosis signals. Our results indicated that TP-containing formulations promoted apoptosis in mouse macrophages, with no significant difference observed between the TP and MPDA-TP groups, and LYP-MPDA-TP exerted the most potent pro-apoptotic effect among these formulations (Figure 4a and b).

Based on the flow cytometry results, we further investigated the impact of LYP-MPDA-TP on apoptosis signaling pathways at the cellular level. As demonstrated in Figure 4c and d, LYP-MPDA-TP significantly enhanced the expression of Caspase 8, consequently activating caspase-3 and suggesting the involvement of the extrinsic pathway in apoptosis. Additionally, we examined Bcl-2 family proteins, including the proapoptotic protein Bax and the antiapoptotic protein Bcl-2 under the treatment of these TP formulations. Our findings revealed a significant reduction in the expression level of Bcl-2 due to LYP-MPDA-TP treatment. This decrease in Bcl-2 subsequently triggered the expression of cytochrome *c* and caspase-9, ultimately leading to mitochondrial dysfunction through the caspase cascade and mitochondrial pathways. Collectively, these results indicate that LYP-MPDA-TP effectively promotes apoptosis in macrophages undergoing pathological changes stimulated by oxLDL. Given that these inflammatory lesion cells play a crucial role in driving sustained progression of AS lesions, LYP-MPDA-TP holds potential for early intervention in AS lesions.

3.5 Effect of LYP-MPDA-TP on the development of cholesterol-rich and high-fat diet-induced AS in ApoE$^{-/-}$ mice

Considering the significant inhibitory effects of LYP-MPDA-TP demonstrated *in vitro* on the polarization of pro-inflammatory M1 macrophages and the downregulation of pro-inflammatory cytokine expression levels, we conducted further investigations to assess the therapeutic efficacy of LYP-MPDA-TP in attenuating AS in ApoE$^{-/-}$ mice induced by a high-cholesterol and high-fat diet. In contrast to previous treatment models, our approach aimed to validate the "prevention at the early stage" strategy for AS therapy. We administered different TP formulations to experimental animals concurrently with the establishment of the animal model, with the objective of achieving early intervention in AS. The experimental procedure is illustrated in Figure 5a.

Histological examination of the aortic root demonstrated a significant inhibition of plaque formation in the LYP-MPDA-TP group compared to the other groups (Figure

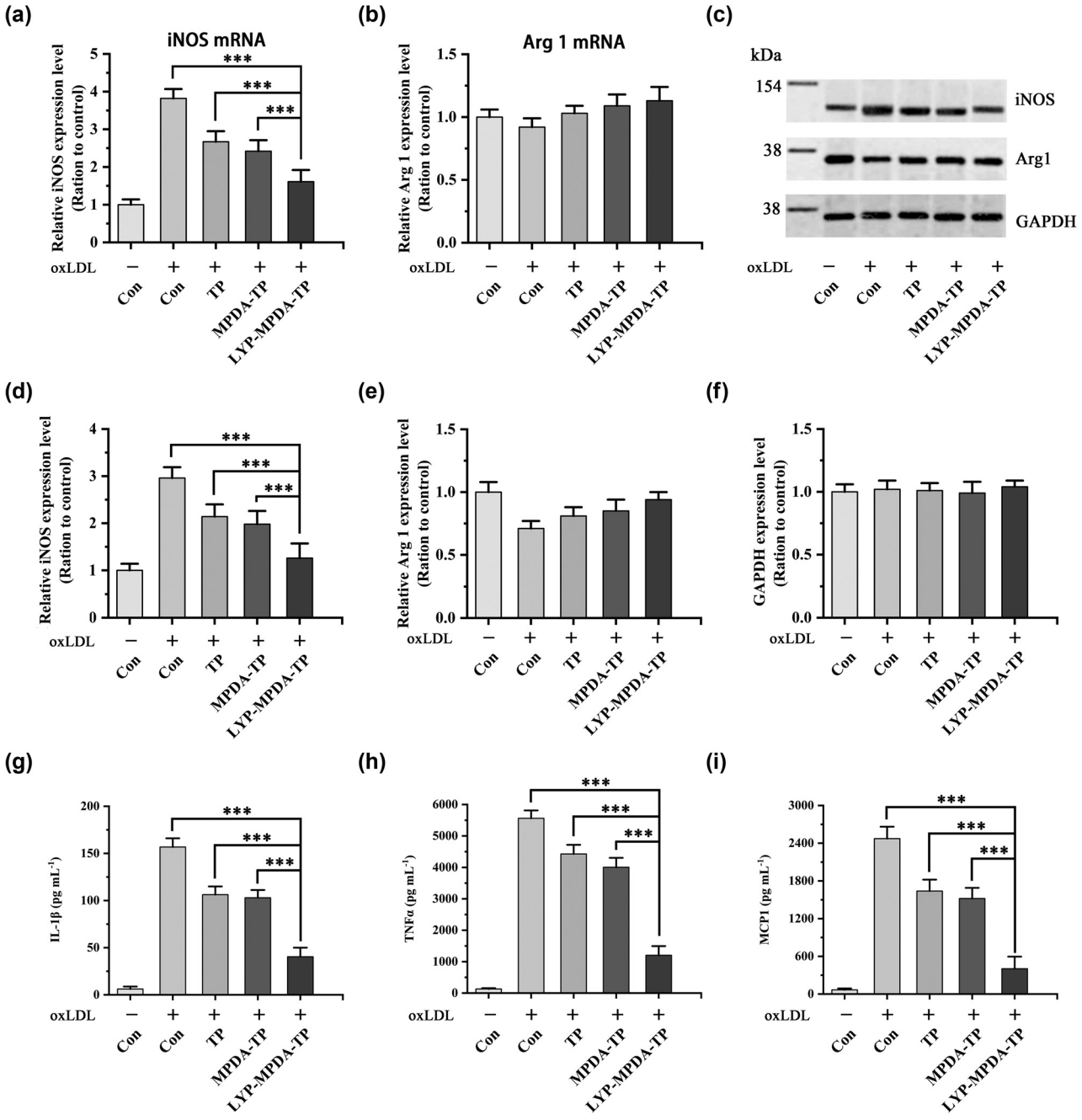

Figure 3: Effects of LYP-MPDA-TP on oxLDL-stimulated macrophage polarization. Mouse RAW264.7 macrophages were co-cultured with oxLDL (50 μg/mL) and various TP formulations (saline, TP, MPDA-TP, LYP-MPDA-TP) for 24 h. The expression levels of phenotypic markers iNOS (M1 macrophages) and Arg1 (M2 macrophages), as well as the corresponding cytokine secretion profiles, were measured. (a and b) RT-PCR analysis of iNOS and Arg1 mRNA levels. (c) Western blot analysis of iNOS and Arg1 protein expression. (d–f) Quantitative analysis of iNOS and Arg1 protein expression using ImageJ software. (g–i) ELISA analysis of TNF-α, IL-6, and MCP-1 levels in the culture supernatant. ***$P < 0.001$.

5b and c). Similarly, the TP and MPDA-TP groups also exhibited plaque inhibition which was consistent with the results of *in vitro* study, although no statistical difference was observed between the two groups. Moreover, we measured the expression levels of inflammatory cytokines in the peripheral blood of the experimental animals, and the results revealed a substantial reduction in the expression levels of total pro-inflammatory cytokines TNFα and IL-1β in the LYP-MPDA-TP group compared to the other groups (Figure 5e and f), approaching levels similar to those observed in the control group mice ($ApoE^{-/-}$ mice on a regular diet, results not shown).

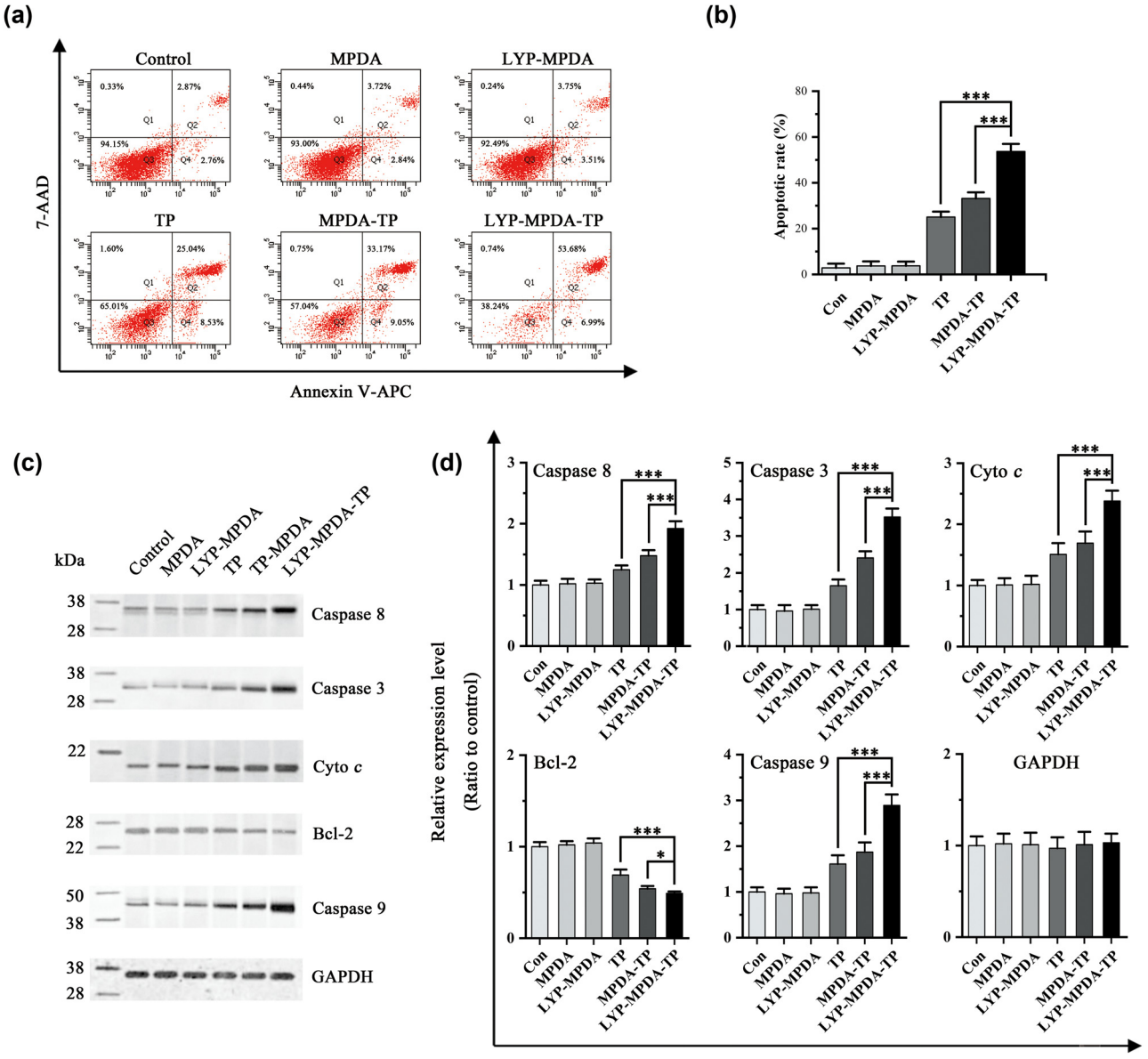

Figure 4: Effects of LYP-MPDA-TP on oxLDL-induced macrophage apoptosis. Mouse RAW264.7 macrophages were co-cultured with oxLDL (50 μg/mL) and various TP formulations (saline, MPDA, LYP-MPDA, TP, MPDA-TP, LYP-MPDA-TP) for 24 h. Macrophage apoptosis was assessed using flow cytometry, and apoptosis signals were evaluated through western blot analysis. (a) Flow cytometry analysis of apoptosis. (b) Quantitative analysis of the cell apoptotic rate using ImageJ software. (c) Western blot analysis of apoptosis-related protein expression. (d) Quantitative analysis of the cell apoptosis-related protein expression using ImageJ software. *$P < 0.05$, ***$P < 0.001$.

4 Discussion

In this study, we developed a nanoparticle delivery system to efficiently load and deliver TP specifically targeting AS macrophages for precise treatment of AS. The delivery system exhibited excellent stability, safety, high encapsulation efficiency, and drug-loading capacity. Effective uptake by target cells and efficient release of the loaded drug are crucial for targeted delivery systems, emphasizing the significance of selecting specific targeting sites.

The loading of active substances by nanoparticles has emerged as a promising approach for the treatment of diseases. For instance, studies have investigated the use of nanoparticles, such as hollow silica nanoparticles and MPDA nanoparticles, to load prohealing peptides like RL-QN15 for skin wound healing [21–23]. These peptide-loaded nanoparticles have demonstrated enhanced therapeutic potential in promoting wound healing compared to the peptides alone, through the slow release of the loaded peptide from the nanoparticles. In this study, we designed a

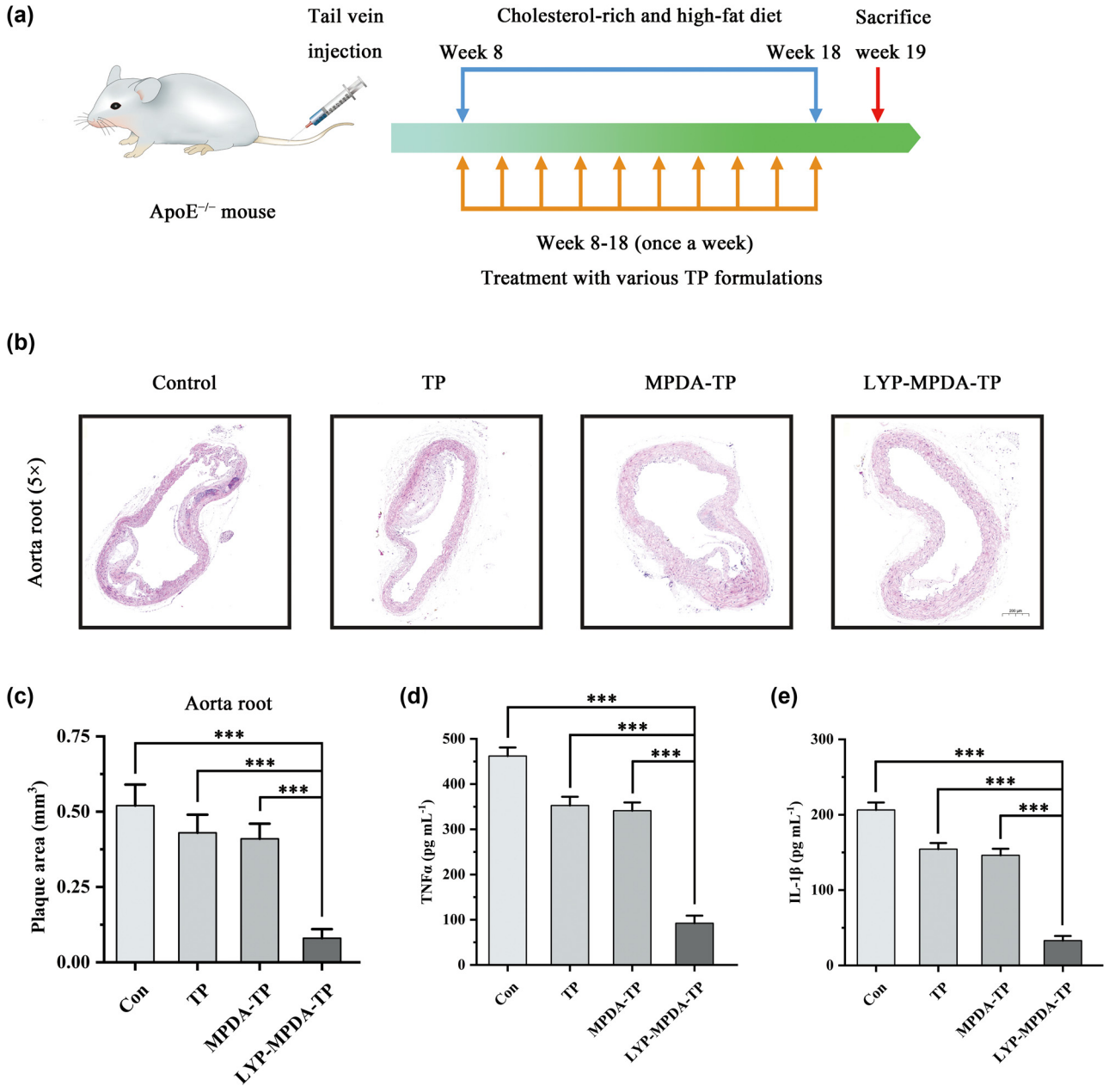

Figure 5: LYP-MPDA-TP ameliorates plaque and inflammation in a cholesterol-rich and high-fat diet-induced atherosclerotic mouse model. (a) Schematic illustration depicting the development of the atherosclerotic mouse model and treatment with various TP formulations (saline, TP, MPDA-TP, and LYP-MPDA-TP). (b–d). Representative photographs and quantitative analysis of H&E-stained sections of the aortic root and aortic arch (n = 6). Scale bar: 500 μm. (e): ELISA analysis of TNF-α, IL-6, and MCP-1 levels in blood serum collected from atherosclerotic mice after treatment with different formulations (saline, TP, MPDA-TP, and LYP-MPDA-TP) at a dose of 2 mg/kg per week (n = 6). All data are presented as mean ± SD. Statistical analysis was performed using one-way ANOVA. ***P < 0.001.

modified MPDA delivery system based on LyP-1 cyclic nonapeptide (LYP-MPDA). It specifically targets macrophages within AS lesions by recognizing the LyP-1 cyclic peptide, facilitating the delivery of TP encapsulated in MPDA to these macrophages [10,17,20]. Consequently, it effectively suppresses the polarization of pro-inflammatory M1 macrophages and reduces the levels of pro-inflammatory factors at the site of inflammation. Moreover, the sustained release and continuous movement of MPDA nanoparticles enable the continuous detection and elimination of aberrant M1 macrophages in the affected regions, potentially further enhancing its anti-atherosclerotic effect [10,17]. The *in vivo* results demonstrated

the remarkable inhibitory effect of LYP-MPDA-TP on the formation of AS.

LyP-1 was initially identified as a tumor-homing peptide with specific recognition for tumor cells, tumor lymphatic vessels, and tumor-associated macrophages, interacting with its receptor protein p32/gC1qR/HABP1 [20]. Previous studies have reported the expression of p32 in atherosclerotic plaques, particularly in macrophages and foam cells, suggesting the therapeutic and diagnostic potential of LyP-1 for AS, as well as a marker for AS vascular macrophages and foam cells [24,25]. Our study demonstrated that foam cells derived from macrophages stimulated by oxLDL displayed excellent targeting uptake efficiency and efficient drug release when treated with LYP-MPDA. Additionally, compared to the challenges encountered in targeting modification in other delivery systems, this study utilized the thiol group in the cysteine residue of the LyP-1 cyclic peptide chain, enabling specific binding to the maleimide on the surface of MPDA. This characteristic facilitated rapid targeting protein modification of the MPDA delivery system, indicating its potential for delivering therapeutic drugs for AS.

To validate the therapeutic effect of LYP-MPDA targeted drug delivery for AS, we selected TP as the candidate drug. Previous studies have confirmed the anti-AS effects of TP through the inhibition of inflammatory reactions and promotion of apoptosis in AS lesion cells *via* activation of the NFκB signaling pathway [26,27]. Consistent with these findings, our *in vitro* experiments demonstrated that LYP-MPDA-TP effectively inhibited M1 polarization of mouse macrophages stimulated by oxLDL, leading to reduced release of pro-inflammatory factors induced by oxLDL compared to pure TP and MPDA-TP. These results suggest the potential of LYP-MPDA-TP for early intervention in AS lesions. Further experiments revealed that LYP-MPDA-TP significantly promoted apoptosis in oxLDL-stimulated lesion macrophages, which play a key role in driving the progression of persistent AS lesions. This finding indicates the potential efficacy of LYP-MPDA-TP in the early intervention of AS lesions.

To further validate the therapeutic efficacy of the delivery system *in vivo*, we established an $ApoE^{-/-}$ atherosclerotic mouse model and compared the effects of different drug formulation combinations. To validate the "preventive" treatment strategy for AS, we administered the corresponding therapeutic drug combinations during the construction of the $ApoE^{-/-}$ atherosclerotic mouse model. The results demonstrated that the LYP-MPDA-TP group exhibited a significantly reduced plaque ratio compared to the pure TP and MPDA-TP groups. Interestingly, while MPDA effectively protected TP, the MPDA-TP group showed a significant difference in plaque size compared to the control group but not compared to the TP group. This further confirms the delivery advantages of the targeted modified delivery system. Therefore, our study suggests that LYP-MPDA-TP may have the potential to slow down and attenuate plaque progression in $ApoE^{-/-}$ mice.

One limitation of our study is the susceptibility of the MPDA nanoparticles used to clearance by the reticuloendothelial system in the body. Despite the successful targeting peptide modification, a certain proportion of nanoparticles encounter challenges in reaching the target cells, which somewhat compromises the delivery efficiency. In future research, we plan to enhance the *in vivo* escape rate of nanoparticles by encapsulating them with biomimetic membranes derived from live cells, thus improving their delivery efficiency. Although a certain proportion of the delivery system in this study is cleared in the body, the therapeutic drugs delivered through it continue to demonstrate excellent *in vitro* and *in vivo* anti-AS treatment effects, highlighting its potential value in targeted drug delivery for AS. Furthermore, a comparative study assessing the half-life of TP and its nanoparticle formulation in the body is warranted. Additionally, a supplementary study evaluating the safety of the nanoparticle formulation, including an assessment of hepatic and renal toxicity through analysis of AST, ALT, Cre, BUN, and histological examination of the liver and kidneys, is recommended. In conclusion, the LyP-1 peptide-modified MPDA nanospheres exhibit excellent targeting ability towards foam cells, effectively inducing apoptosis, and inhibiting their proliferation, invasion, and migration. Additionally, they demonstrate good biocompatibility. These findings provide a crucial theoretical basis and methodological reference for the design of targeted delivery systems for anti-AS nanoparticles, offering a new approach for the treatment of AS. Future studies should focus on optimizing the formulation of the delivery system and further investigating its safety and efficacy in animal models and clinical trials.

Funding information: This work was supported by the National Natural Science Foundation of China (No. 81770285, No. 31871152, No. 81971328, No. 82271624) and the Natural Science Foundation of Hebei Province of China (No. H2022206074, No. H2021206459).

Author contributions: Lei Zheng, Xinhua Zhang, and Jinkun Wen were responsible for the conception and design of the study. Qianfan Zhang, Hongguang Lian, Wenli Wang, Liangsheng Li, and Zekun Zhen contributed to the experiment performance and data collection. Ziyan Li, Lingdan Zhao, Tingting Zhang, and Wei Zhang were responsible for the statistical analysis. All authors have accepted

responsibility for the entire content of this manuscript and approved its submission.

Conflict of interest: The authors state no conflict of interest.

Data availability statement: The datasets generated and/or analyzed during the current study are available from the corresponding author on reasonable request.

References

[1] Falk E. Pathogenesis of atherosclerosis. J Am Coll Cardiol. 2006;47:C7–12.

[2] Libby P. The changing landscape of atherosclerosis. Nature. 2021;592(7855):524–33.

[3] Libby P, Bornfeldt KE, Tall AR. Atherosclerosis: Successes, Surprises, and Future Challenges. Circ Res. 2016;118(4):531–4.

[4] Kasikara C, Doran AC, Cai B, Tabas I. The role of non-resolving inflammation in atherosclerosis. J Clin Invest. 2018;128(7):2713–23.

[5] Koelwyn GJ, Corr EM, Erbay E, Moore KJ. Regulation of macrophage immunometabolism in atherosclerosis. Nat Immunol. 2018;19(6):526–37.

[6] Colin S, Chinetti-Gbaguidi G, Staels B. Macrophage phenotypes in atherosclerosis. Immunol Rev. 2014;262(1):153–66.

[7] Eshghjoo S, Kim DM, Jayaraman A, Sun Y, Alaniz RC. Macrophage polarization in atherosclerosis. Genes (Basel). 2022;13(5):756.

[8] Fadini GP, Simoni F, Cappellari R, Vitturi N, Galasso S, Vigili de Kreutzenberg S, et al. Pro-inflammatory monocyte-macrophage polarization imbalance in human hypercholesterolemia and atherosclerosis. Atherosclerosis. 2014;237(2):805–8.

[9] Barrett TJ. Macrophages in Atherosclerosis Regression. Arterioscler Thromb Vasc Biol. 2020;40(1):20–33.

[10] Chen W, Schilperoort M, Cao Y, Shi J, Tabas I, Tao W. Macrophage-targeted nanomedicine for the diagnosis and treatment of atherosclerosis. Nat Rev Cardiol. 2022;19(4):228–49.

[11] Bonfiglio CA, Weber C, Atzler D, Lutgens E. Immunotherapy and cardiovascular diseases: novel avenues for immunotherapeutic approaches. QJM. 2023;116(4):271–8.

[12] Aghamajidi A, Gorgani M, Shahba F, Shafaghat Z, Mojtabavi N. The potential targets in immunotherapy of atherosclerosis. Int Rev Immunol. 2023;42(3):199–216.

[13] Weber C, Noels H. Atherosclerosis: current pathogenesis and therapeutic options. Nat Med. 2011;17(11):1410–22.

[14] Liu H, Zhu L, Chen L, Li L. Therapeutic potential of traditional Chinese medicine in atherosclerosis: A review. Phytother Res. 2022;36(11):4080–100.

[15] Wang C, Niimi M, Watanabe T, Wang Y, Liang J, Fan J. Treatment of atherosclerosis by traditional Chinese medicine: Questions and quandaries. Atherosclerosis. 2018;277:136–44.

[16] Song CY, Xu YG, Lu YQ. Use of Tripterygium wilfordii Hook F for immune-mediated inflammatory diseases: progress and future prospects. J Zhejiang Univ Sci B. 2020;21(4):280–90.

[17] Lin K, Gan Y, Zhu P, Li S, Lin C, Yu S, et al. Hollow mesoporous polydopamine nanospheres: synthesis, biocompatibility and drug delivery. Nanotechnology. 2021;32(28):285602.

[18] Uchida M, Kosuge H, Terashima M, Willits DA, Liepold LO, Young MJ, et al. Protein cage nanoparticles bearing the LyP-1 peptide for enhanced imaging of macrophage-rich vascular lesions. ACS Nano. 2011;5(4):2493–502.

[19] Seo JW, Baek H, Mahakian LM, Kusunose J, Hamzah J, Ruoslahti E, et al. 64Cu-labeled LyP-1-dendrimer for PET-CT imaging of atherosclerotic plaque. Bioconjug Chem. 2014;25(2):231–9.

[20] Song N, Zhao L, Zhu M, Zhao J. Recent progress in LyP-1-based strategies for targeted imaging and therapy. Drug Delivery. 2019;26(1):363–75.

[21] Qin P, Tang J, Sun D, Yang Y, Liu N, Li Y, et al. Zn(2+) Cross-Linked Alginate Carrying Hollow Silica Nanoparticles Loaded with RL-QN15 Peptides Provides Promising Treatment for Chronic Skin Wounds. ACS Appl Mater Interfaces. 2022;14(26):29491–505.

[22] Qin P, Meng Y, Yang Y, Gou X, Liu N, Yin S, et al. Mesoporous polydopamine nanoparticles carrying peptide RL-QN15 show potential for skin wound therapy. J Nanobiotechnology. 2021;19(1):309.

[23] Fu Z, Sun H, Wu Y, Li C, Wang Y, Liu Y, et al. A cyclic heptapeptide-based hydrogel boosts the healing of chronic skin wounds in diabetic mice and patients. NPG Asia Materials. 2022;14:99.

[24] She ZG, Hamzah J, Kotamraju VR, Pang HB, Jansen S, Ruoslahti E. Plaque-penetrating peptide inhibits development of hypoxic atherosclerotic plaque. J Control Release. 2016;238:212–20.

[25] Hamzah J, Kotamraju VR, Seo JW, Agemy L, Fogal V, Mahakian LM, et al. Specific penetration and accumulation of a homing peptide within atherosclerotic plaques of apolipoprotein E-deficient mice. Proc Natl Acad Sci U S A. 2011;108(17):7154–9.

[26] Song C, Wang Y, Cui L, Yan F, Shen S. Triptolide attenuates lipopolysaccharide-induced inflammatory responses in human endothelial cells: involvement of NF-kappaB pathway. BMC Complement Altern Med. 2019;19(1):198.

[27] Qiu D, Kao PN. Immunosuppressive and anti-inflammatory mechanisms of triptolide, the principal active diterpenoid from the Chinese medicinal herb Tripterygium wilfordii Hook. f. Drugs R D. 2003;4(1):1–18.